

The transmission of the acoustic wave in the quasi one-dimensional multi-layer systems

**K. Gruszka^{a,*}, S. Garus^a, M. Nabiałek^a, K Błoch^a,
J. Gondro^a, M. Szota^b, B. Pająk^c**

^a Institute of Physics, Technical University of Częstochowa,
ul. Armii Krajowej 19 42-200 Częstochowa, Poland

^b Institute of Materials Engineering, Technical University of Częstochowa,
ul. Armii Krajowej 19, 42-200 Częstochowa, Poland

^c Department of Production Management and Logistics, Technical University
of Częstochowa, ul. Armii Krajowej 19, 42-200 Częstochowa, Poland

* Corresponding e-mail address: kgruszka@wip.pcz.pl

Received 20.10.2013; published in revised form 01.12.2013

Properties

ABSTRACT

Purpose: Paper presents the results of the simulation of acoustic wave propagation in quasi one-dimensional multi-layered structure. The purpose was to examine the influence of the thickness of two materials forming the transmission system, depending on the acoustic wave source frequency.

Design/methodology/approach: To perform simulation, the FDTD (finite difference time domain) algorithm was used. An acoustic wave propagated through the system consisting of ten alternating layers of equal thickness, surrounded on both sides by air. On the edges of the simulation space Neumann boundary conditions were provided.

Findings: Changing the layer thickness affects the position of the SPL minima and causes narrowing of the area of the total acoustic pressure curves.

Research limitations/implications: The influence of changes in the thickness of the layers forming the quasi one-dimensional multilayer system on transmission was investigated. In order to better know the transmission characteristics of the system consisting of two different materials, the effect of changing the physical size of heterogeneous layers should be examined. It would be also important to compare the simulation results with those obtained experimentally.

Practical implications: Simulation of quasi one-dimensional multi-layer systems allows to design new materials adapted to the requirements of specific applications without the need to carry experiment. Multilayer systems can be operated in a variety of applications, primarily as a filter with adjustable band gap frequency intermittently, and also as a material for absorbing incident acoustic waves.

Originality/value: The available literature contains a limited information on the propagation of acoustic waves in quasi one-dimensional multi-layer systems. This paper responds to the demand caused by the lack of available articles in this topic and enables view the findings of research for one of the simpler periodic structures.

Keywords: FDTD, quasi-one-dimensional multilayers, acoustic wave propagation, frequency domain

Reference to this paper should be given in the following way:

K. Gruszka, S. Garus, M. Nabiałek, K Błoch, J. Gondro, M. Szota, B. Pająk, The transmission of the acoustic wave in the quasi one-dimensional multi-layer systems, Journal of Achievements in Materials and Manufacturing Engineering 61/2 (2013) 250-256.

1. Introduction

FDTD method is increasingly used in simulations of acoustic wave propagation, as compared to other type of approach and allows to perform calculations in a relatively short period of time while ensuring a good accuracy of the calculation. For this reason, simulations of simple one-dimensional structures are burdened with insignificant error, since the use of highly accurate computational grids dividing experimental space does not result in a drastic increase in the duration of the simulation.

Quasi one-dimensional multi-layer systems are also extensively studied using the FDTD method particularly in terms of transmission ability for a wide spectrum of electromagnetic radiation [1,2]. In the available literature there is few information on the studies using this method for the transmission properties of superlattices, when the wave incident on the system is an acoustic wave. Systems of this type have interesting physical properties, also from the point of view of application. There are so-called band gaps or certain frequency bands for which the acoustic wave is completely suppressed within the multilayer system, and not leave it. [1-3]. Width, location and total number of forbidden band gaps is strongly correlated with the physical properties of the multilayer system and the topology of its components [1,2]. Such systems can be used, inter alia, as a frequency filters, suitable for the suppression of selected, specific frequency ranges, and also to dampen acoustic wave as the absorbing layer.

For example in reduce level of sound volume, usually used specially shaped materials that act on the basis of scattering of the incident acoustic wave in different directions, and thereby realize a reduction in sound pressure level. The overall effectiveness of this scattering is proportional to the surface area and the amount of planes located on such material. In order to maximize the dissipation is necessary to use elements of considerable significant physical size. Sometimes it is not possible to use such materials e.g. because of their not suitable appearance. What emerges is a need to seek other new solutions that could efficiently meet this challenge.

2. Theoretical background

FDTD method allows to simulate acoustic wave propagation in any medium [4] and is widely used in many experiments related to acoustic simulations [3,5,7,8,9,11].

To describe the behavior of the acoustic wave in the specific medium, it is necessary to come out of the first order differential equations [10]:

$$\kappa \frac{\partial}{\partial t} p(\hat{x}, t) = \nabla \cdot \hat{u} \quad (1)$$

$$\rho_0 \rho_r \frac{d}{dt} \hat{u}(\hat{x}, t) = \nabla p(\hat{x}, t) \quad (2)$$

where:

$p(\hat{x}, t)$ - is the pressure field

$[F / m^2] = [kg / (m \cdot sec^2)]$,

$\hat{u}(\hat{x}, t)$ - is the velocity vector $[m / s]$,

ρ_0 - is the medium density,

ρ_r - is a relative density with respect to the ρ_0 ,

κ - is the medium compressibility $\kappa = 1 / (\rho_0 \cdot \rho_r \cdot c^2)$,

c - is the speed of sound in medium.

Equation (1) for the general case can be written as follows:

$$\frac{\partial p(x, y, z, t)}{\partial t} = \frac{1}{\kappa(x, y, z)} \left[\frac{\partial u_x(x, y, z, t)}{\partial x} + \frac{\partial u_y(x, y, z, t)}{\partial y} + \frac{\partial u_z(x, y, z, t)}{\partial z} \right] \quad (3)$$

In analogy with the FDTD algorithm for electromagnetic wave, Yee cell is defined for the acoustic wave [6,10]. However, they are not identical and the difference lies in other arrangement of the velocity vector components in the interstitial positions, while the scalar pressure field values are in the nodes of the cell.

To describe the propagation of acoustic waves in the Yee cell, equations (1) and (2) should be differentiated over time and space. After differentiation those equations, we obtain the following formula:

$$p^{n+1/2}(i, j, k) = p^{n-1/2}(i, j, k) + \frac{\Delta t \cdot \rho_0 \rho_r c^2}{\Delta x} \cdot [u_x^n(i+1/2, j, k) - u_x^n(i-1/2, j, k)] + \frac{\Delta t \cdot \rho_0 \rho_r c^2}{\Delta y} \cdot [u_y^n(i, j+1/2, k) - u_y^n(i, j-1/2, k)] + \frac{\Delta t \cdot \rho_0 \rho_r c^2}{\Delta z} \cdot [u_z^n(i, j, k+1/2) - u_z^n(i, j, k-1/2)] \quad (3)$$

$$u^{n+1/2}(i, j, k) = u^{n-1/2}(i, j, k) + \frac{\Delta t}{\rho_r(i+1/2, j, k) \cdot \rho_0 \cdot \Delta x} \cdot [p^n(i+1, j, k) - p^n(i, j, k)] + \frac{\Delta t}{\rho_r(i, j+1/2, k) \cdot \rho_0 \cdot \Delta y} \cdot [p^n(i, j+1, k) - p^n(i, j, k)] + \frac{\Delta t}{\rho_r(i+1/2, j, k+1/2) \cdot \rho_0 \cdot \Delta z} \cdot [p^n(i, j, k+1) - p^n(i, j, k)] \quad (4)$$

In equations (3) and (4) n is a step in three-dimensional space $\{p, u\}$ made by pressure field $p(\hat{x}, t)$ and velocity field $\hat{u}(\hat{x}, t)$. The grid formed by a given field can be a square grid, ie. $\Delta x = \Delta y$ or more often a triangular mesh, which can shorten the calculation time because of its special arrangement to significant density of nodes only in areas close to the interesting from the point of view of the experimenter.

These patterns are general solutions used in the case when considering the problem localized in three-dimensional space. For the quasi one-dimensional case, studied in this work, an restriction can be made to examine only one-dimensional problem, described by the following equation:

$$p^{n+1/2}(k) = p^{n+1/2} + ga(k) \cdot [u_d^n(k+1/2) - u_d^n(k-1/2)] \quad (5)$$

$$u_d^{n+1/2}(k+1/2) = u_d^n(k+1/2) + gb(k+1/2) \cdot [p^{n+1/2}(k+1) - p^{n+1/2}(k)] \quad (6)$$

where: d is one of the preferred axis of the system such as z-axis while:

$$ga(k) = \frac{\Delta t \cdot \rho_0 \rho_r \cdot c^2}{\Delta d}, \quad (7)$$

$$gb(k+1/2) = \frac{\Delta t}{\Delta d \cdot \rho(k+1/2) \cdot \rho_0 \cdot c^2 \cdot \Delta d} \quad (8)$$

It is very important, that the time step Δt that appears in the above differential equations, has been chosen in such a way, that with the minimum value does not restrict overly the entire simulation speed. The same rule applies to the spatial step Δd . Choosing this parameter should be aware of the Courant's stability condition [10], which for simulation in three-dimensional space is defined as follows:

$$c\Delta t \leq \frac{1}{\sqrt{(1/\Delta x)^2 + (1/\Delta y)^2 + (1/\Delta z)^2}} \quad (9)$$

while for the case of one-dimensional problem, it shall be adopted on a simplified form:

$$c\Delta t \leq \frac{1}{\sqrt{(1/\Delta d)^2}} \quad (10)$$

Courant's stability condition ensures, that the simulation will be stable and convergent, and during the course of an iterative algorithm does not see any artifacts associated with a bad choice of space or time steps.

3. Simulation setup

Fig. 1 shows the structure of the model simulation performed using the FDTD method. Quasi one-dimensional multilayer structure (a structure in which only one of the dimensions is finite and the others tend to infinity) was formed with an alternate stacking of two types of thin films. As the material A aluminum foil was used, while as material B polypropylene film was used. Both materials have the same thickness d and directly adjacent to each other in such a way, that they formed a periodic translationally invariant structure of a 10 elements in total, that made up the layers of the superlattice. This superlattice is surrounded by a layer of air on both sides, wherein one side provided with an acoustic source emits a acoustic plane wave directly into the corresponding air. Key parameters for the simulation, adopted for each medium are summarized in Table 1.

Table 1. Some key properties of used mediums / materials

Medium	Speed of sound [m/s]	Density [kg/m ³]
air	343	1.2
aluminum	6300	2700
polypropylene	1200	900

At both ends of the simulation the so-called hard boundary conditions (Neumann boundary condition) were provided, and are described by the following relation:

$$-\hat{n} \cdot \left(-\frac{1}{\rho c} \nabla p - \hat{q} \right) = 0 \quad (11)$$

where: \hat{n} - is the normal vector to boundary plane.

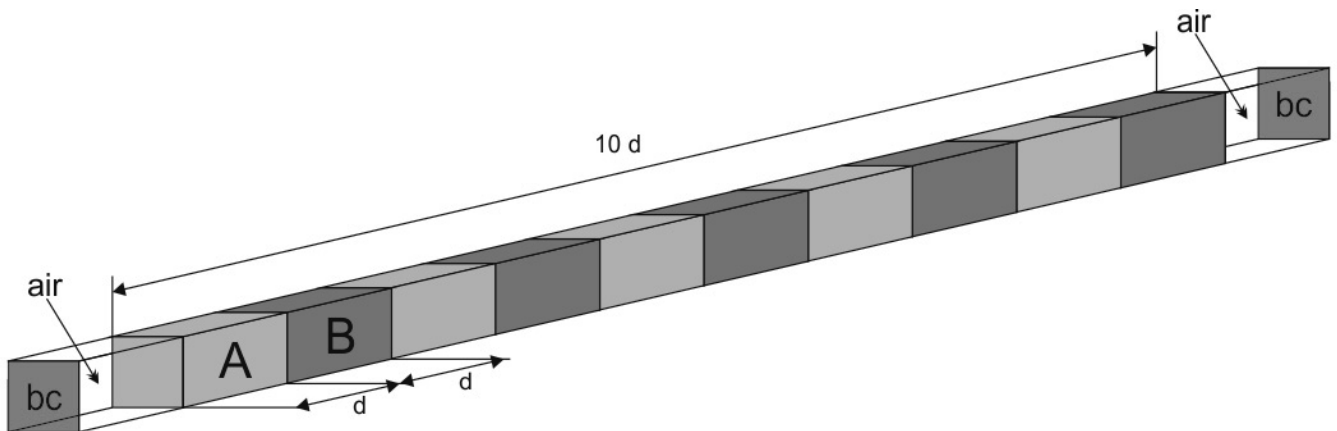


Fig. 1. Model used in simulation. A - aluminum, B - polypropylene, bc - Neumann boundary conditions, d - length of element

The simulation is performed in the frequency domain, whereby it became possible to study the frequency response of the system, and to investigate the properties of the individual damping layers.

After the initial simulation, it was decided, that the range within which a detailed analysis will be carried out was limited to the range from 200 Hz to 5 kHz, because due to the phenomena occurring in, it was definitely the most interesting from the physics point of view. In the case of lower or higher frequencies, basically they passed smoothly or were completely absorbed by the multilayer structure.

The simulations were performed for the ambient temperature of 293.15 K with the initial reference pressure of 1 atm. Computing grid applied to the experimental space consisted of 118 points distributed evenly in all layers of the studied superlattice, and in the surrounding air medium.

Air-filled space surrounding the studied structure was always the same size, and was fixed to 5 mm in thickness.

4. Results

In this work, the influence of the thickness *d* of layers composed of alternating materials A and B to the acoustic wave transmission was studied. The thickness of the materials was changed in the range from 0.5 mm to 1.0 mm with the step 0.1 mm.

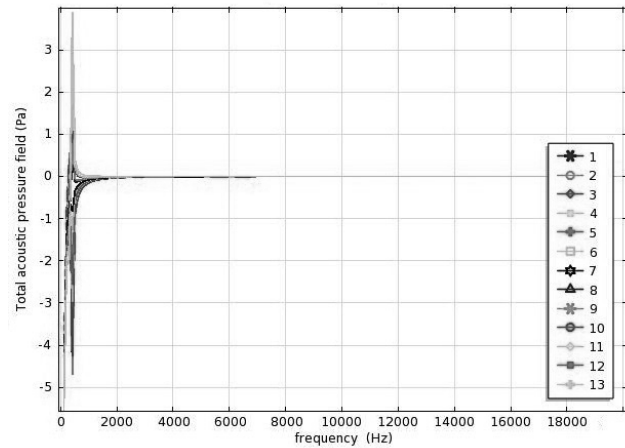


Fig. 2. Total acoustic pressure in function of frequency. Numbers 2 - 12 indicate layer number, thickness *d*=0.5 mm

Figs. 2 and 3 show the total acoustic pressure as a function of frequency for the thickness of the layers *d*=0.5 mm. Numbers 1 and 13 stands for the areas filled with air, while the numbers from 2 to 12 indicate subsequent layers, starting from material A, as it is shown in Fig. 1. Above frequency of approximately 2 kHz, the sound pressure curves converge to a value close to 0 Pa, and thus to ambient pressure. Above 7 kHz, frequency curves reach 0 Pa for all layer thicknesses *d* in the studied range up to 1 mm. For this reason, the calculation frequency range has been limited to 5 kHz, and simulations were then carried out for further analysis.

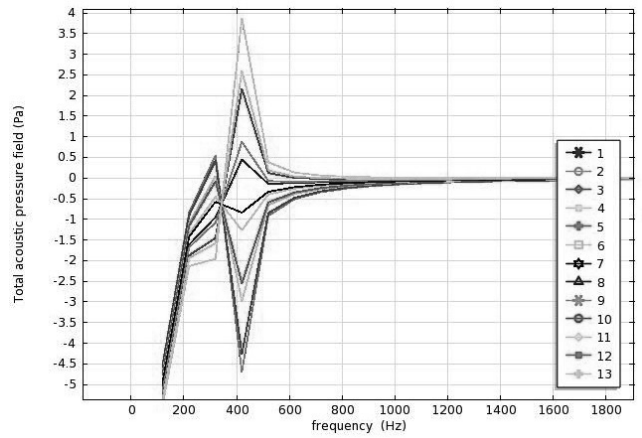


Fig. 3. Closeup of Fig. 1. in the frequency range between 150 Hz-1.8 KHz

As can be seen in Fig. 2, the total acoustic pressure curves show an interesting course. Near frequency of approximately 200 Hz, the curves begin to diverge in order to achieve a first maximum in the frequency of 316 Hz. Then, in frequency 325 Hz, acoustic pressure curves converge again, and there is a exchange in position of some of them. From this point, some of them (the layers numbered 8-11) again tends to a maximum that occurs at a frequency of 420 Hz. Then, accurately 100 Hz higher, curves achieve the point at which acoustic pressure decreases more slowly, until the limit frequency of 7 kHz.

Fig. 4 provided SPL pressure curves (sound pressure level) expressed in dB for structures with layer thicknesses *d*=0.5 mm.

The SPL pressure level is defined as:

$$SPL = 10 \log \left\langle \frac{p^2}{p_0^2} \right\rangle \tag{12}$$

where:

$\langle p^2 \rangle$ - is the mean square of sound pressure;

$p_0 = 2 \cdot 10^{-5} [Pa]$ - is the reference pressure value.

On the acoustic wave transmission shown in Fig. 4, the visible SPL minima is exceeding slightly above half of the thickness of the entire multilayer system. Acoustic wave leaving the examined structure is more suppressed, the higher is the frequency of wave source. As a result of the constructive interference phenomena, for the highest of the transmitted wave length (frequency 200 Hz) there is a slight strengthening of the sound level after leaving the structure. Furthermore, as the frequency of the sound increases, the further in the direction of increasing *x*-coordinate values of location the minimum occurs.

Below, in the Fig. 5 shows the total acoustic pressure curves versus frequency for the structure of which the thickness *d* = 0.5 mm, focusing only on the limited to 5 kHz area of the calculations.

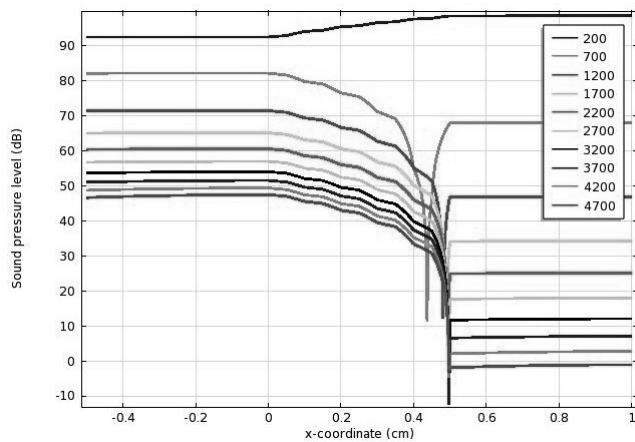


Fig. 4. Sound pressure level in function of x coordinate for thickness $d=0.5$ mm. Legend shows frequency in [Hz]

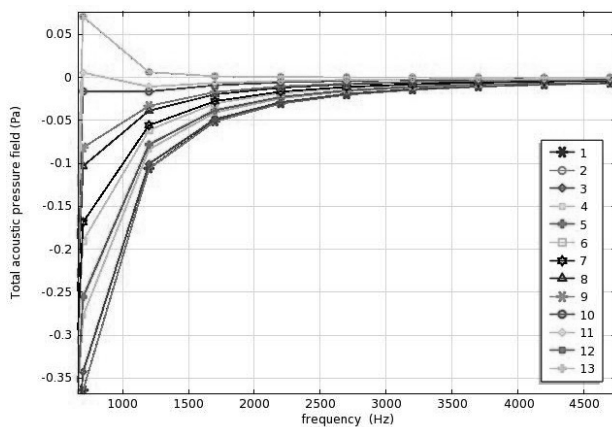


Fig. 5. Total acoustic pressure [Pa] in function of frequency. Numbers 2 - 12 indicate layer number, thickness $d=0.5$ mm

Fig. 6 shows the sound pressure level curves for the structure of the individual components thickness was $d=0.6$ mm.

Increasing the thickness of the individual layers only by 1 mm, resulted in a shift of all the frequency minima in the direction of the x coordinate, increasing their position relative to the structure in which was $d=0.5$ mm.

Table 2 sums up the SPL curve parameters for the frequency of 700 Hz, depending on the layer thickness d of the studied structure.

There was only a slight change in the initial intensity of total acoustic pressure curves for superlattice layers numbered 2-7 amounting -0.01 Pa. For layers number from 8 to 11, the same change of pressure value occurred in the direction of increasing sound pressure.

In Figs. 8-11 the total acoustic pressure curves (Fig. 8 and Fig. 10) and the SPL sound pressure level curves (Fig. 9 and Fig. 11) are shown, for multilayer structures with thicknesses

d respectively of $d=0.9$ mm and $d=1.0$ mm. For structures with values of thickness $d = 0.7$ mm and $d = 0.8$ mm the results of the acoustic wave transmission for the total acoustic pressure level and SPL sound pressure level were basically the same, as for layer thicknesses in the range of $d = 0.5$ mm and $d = 0.9$ mm. It was found that for the entire range of investigated thickness, shifts in the location of the SPL minimum vary linearly, shifting in the direction opposite to the end where the sound wave source is located. Have also been identified an increasing dependency for the difference in levels of sound pressure level of wave entering the structure SPL_{in} and wave leaving the test structure SPL_{out} .

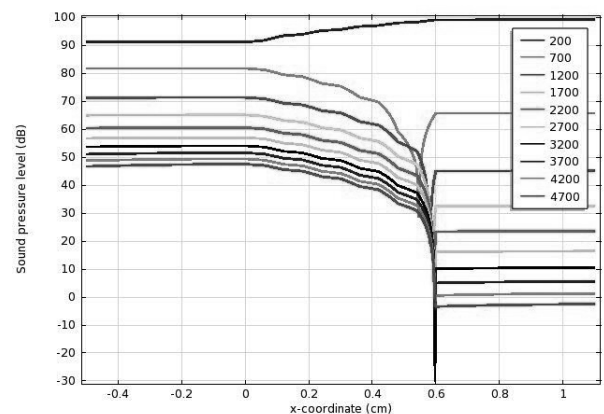


Fig. 6. Sound pressure level in function of x coordinate for thickness $d=0.6$ mm. Legend shows frequency in [Hz]

Table 2.

Parameters change of 700 Hz curve taken from SPL for different thickness d

Thickness d [mm]	$SPL_{in} - SPL_{out}$ [dB]	Minimum location [mm]
0.5	14.20	0.437
0.6	16.05	0.545
0.7	17.55	0.644
0.8	18.89	0.746
0.9	20.00	0.846
1.0	21,02	0.946

Fig. 7 shows total acoustic pressure curves for structure layers of thicknesses $d=0.6$ mm

As can be seen in Fig. 10, there is a curve having a minimum frequency of 200 Hz. A previously unobserved minimum is the result of interference of waves reflected from the various inner layers, which imposition resulted in the interference with the wave reflected from the last layer. On the occurrence of the SPL minima also standing waves that appear in the test structure have significant influence.

Figs. 9 and 11 present the total acoustic pressure for with a layer thickness are respectively $d=0.9$ mm and $d=1.0$ mm. As expected, there was narrowing of the total acoustic pressure, and the curves specified previously which are describing layers numbered 2-7 tend towards negative values of the total pressure, and curves numbered 8-11 move towards positive values.

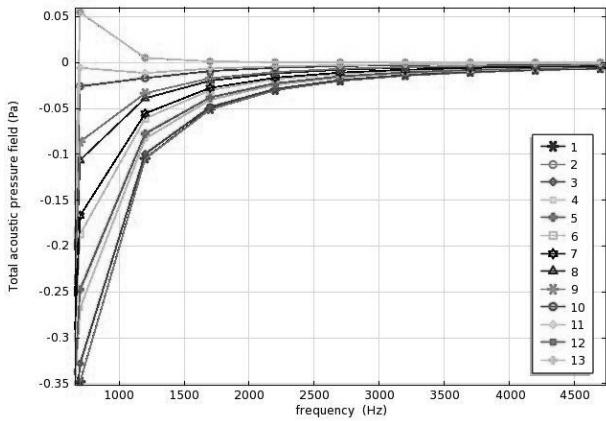


Fig. 7. Total acoustic pressure [Pa] in function of frequency. Numbers 2 - 12 indicate layer number, thickness $d=0.6$ mm

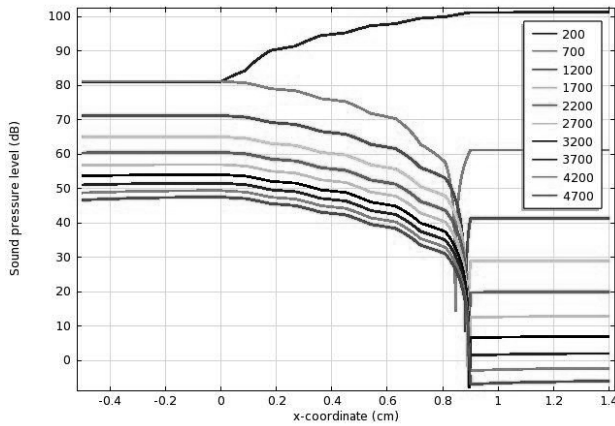


Fig. 8. Sound pressure level in function of x coordinate for thickness $d=0.9$ mm. Legend shows frequency in [Hz]

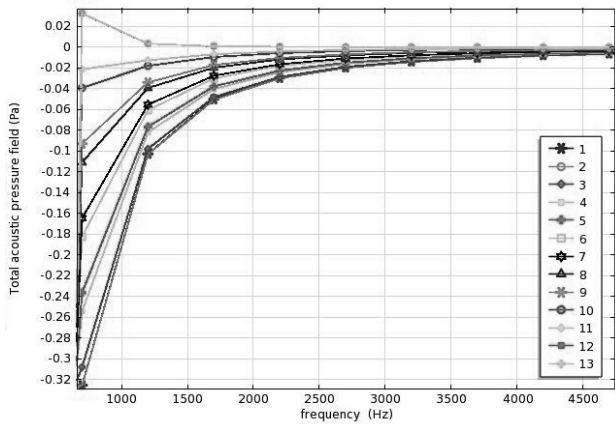


Fig. 9. Total acoustic pressure [Pa] in function of frequency. Numbers 2 - 12 indicate layer number, thickness $d=0.9$ mm

Size of the space filled by air, marked on all charts by numbers 1 and 13, remained constant fixed to 5 mm. Although the thickness of

these layers is not changed over the entire simulation, also in these areas, the initial value of the sound pressure curve decrease. This is caused by reflection of the acoustic wave part of the first and subsequent layers of the system, which causes the phenomenon of interference with the wave emitted from the source.

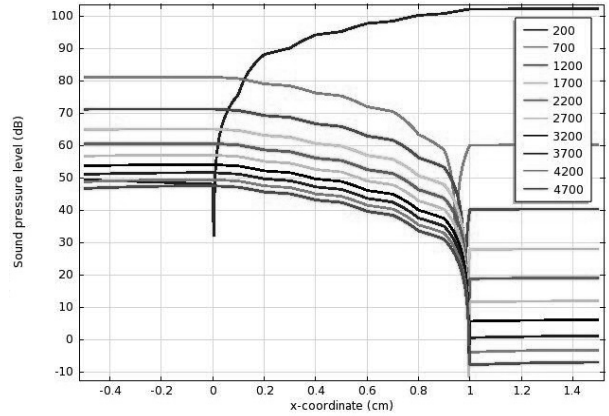


Fig. 10. Sound pressure level in function of x coordinate for thickness $d=1.0$ mm. Legend shows frequency in [Hz]

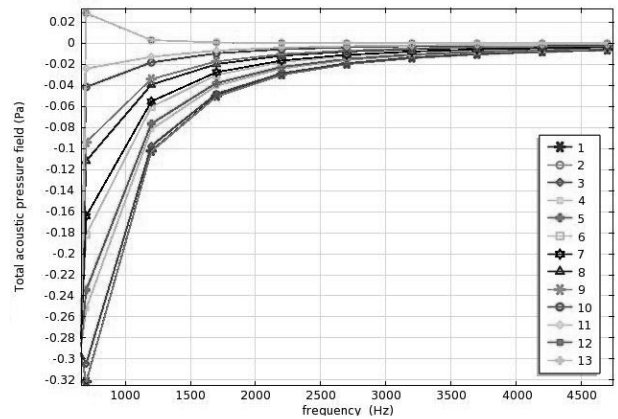


Fig. 11. Total acoustic pressure [Pa] in function of frequency. Numbers 2 - 12 indicate layer number, thickness $d=1.0$ mm

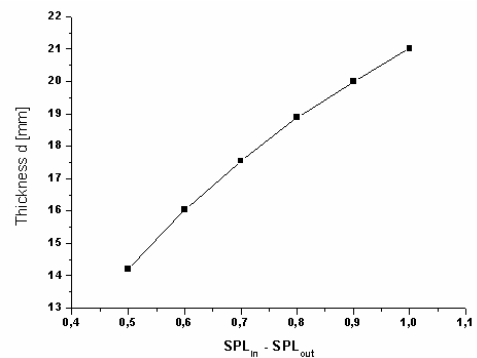


Fig. 12. $SPL_{in} - SPL_{out}$ shift dependency for 700 Hz curve

Fig. 12 and Fig. 13, show the relationship of SPL movement and offset of minimum localisation based on the thickness d of a layer system presented in Figs. 4, 6, 8 and 10 for 700 Hz sound pressure level curve.

For the curve from Fig. 12, the fit of factors was made, according to the quadratic equation:

$$f(x) = a \cdot x^2 + b \cdot x + c \quad (13)$$

The obtained fitting coefficients are: $a=-10.1964$, $b=28.8061$, $c=2.38$.

Also, for the curve from Fig. 13, a linear fit was performed in accordance with the relationship:

$$f(x) = a \cdot x + b \quad (14)$$

The calculated fitting factors are: $a=1.0142$, $b=-0.0667$.

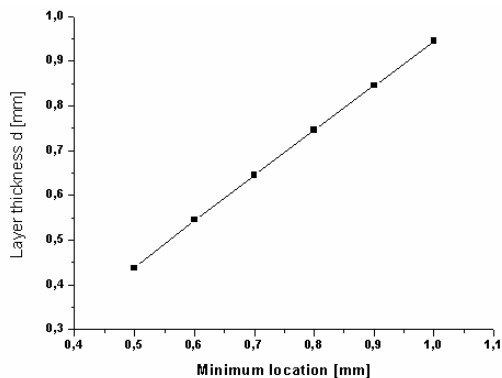


Fig. 13. Minimum location shift for 700 Hz curve, dependency

5. Conclusions

In this paper the acoustic wave transmission by a quasi-one-dimensional multi-layer structure depending on the thickness of each layer was studied. For the examined structure, a series of graphs depicting the dependence of the total acoustic pressure level and sound pressure level was obtained. As the thickness of the layers increase, narrowing range of sound pressure curves occurs and the shift of SPL minimum is observed.

Also, it was determined that fitting dependency of sound pressure level minimum shift was found to be linear, and the difference between SPL_{in} - SPL_{out} is defined by the second degree polynomial function.

References

- [1] J. Garus, S. Garus, K. Gruszka, R. Hrański, Studies of transmission abilities of permutations of three-layer structures in visible light, *New Technologies and Achievements in Metallurgy and Materials Engineering, A Collective Monograph* (2012) 764-767.
- [2] S. Garus, J. Garus, K. Gruszka, Emulation of electromagnetic wave propagation in superlattices using FDTD algorithm, *New Technologies and Achievements in Metallurgy and Materials Engineering, A Collective Monograph* (2012) 768-771.
- [3] Z. Zhan, P. Wei, Influences of anisotropy on band gaps of 2D phononic crystal, *Acta Mechanica Solida Sinica* 23/2 (2010) 181-188.
- [4] Hong Wei Yang, Ze Kun Yang, Jian Xiao Liu, Ai Ping Li, Xiong You, A novel DGS microstrip antenna simulated by FDTD, *Optik* 124/16 (2013) 2277-2260.
- [5] Y. Pennec, J.O. Vasseur, B. Djafari-Rouhani, L. Dobrzyński, P.A. Deymier, Two-dimensional phononic crystals, Examples and application, *Surface Science Reports*, 65/8 (2010) 229-291.
- [6] K. Yee, Numerical solution of initial boundary value problems involving Maxwell's equations in isotropic media, *IEEE Transactions on Antennas and Propagation* 14/3 (1966) 302-307.
- [7] J. Lovetri, D. Mardare, G. Souloudre, Modeling of the seat dip effect using the finite-difference time-domain method *Journal of the Acoustical Society of America* 100 (1996) 2204-2212.
- [8] A. Chaigne, A. Askenfelt, Numerical simulations of piano strings-Part I: a physical model for a struck string using finite difference methods, *Journal of the Acoustical Society of America* 95/2 (1994) 1112-1118.
- [9] V. Ostashev, D. Wilson, L. Liu, D. Aldridge, N. Symons, D. Marlin, Equations for finite-difference time-domain simulation of sound propagation in moving inhomogeneous media and numerical implementation *Journal of the Acoustical Society of America* 117 (2005) 503-517.
- [10] D.M. Sullivan, *Electromagnetic simulation using the FDTD method*, IEEE Press, 2000.
- [11] J.G. Maloney, K.E. Cummings, Adaptation of FDTD techniques to acoustic modeling, *11th Annual Review of Progress in Applied Computational Electromagnetics* 2 (1995) 724-731.
- [12] C. Spa, A. Garriga, J. Escolano, Impedance boundary conditions for pseudo-spectral time-domain methods in room acoustics, *Applied Acoustics* 71/5 (2010) 402-410.